

2005

Relationship between the extent of non-viable myocardium and regional left ventricular function in chronic ischemic heart disease

Arunark Kolipaka

Cleveland Clinic Foundation and Cleveland State University

George P. Chatzimavroudis

Cleveland State University

Richard D. White

Cleveland Clinic Foundation


Michael L. Lieber

Cleveland Clinic Foundation

Randolph M. Setser

Cleveland Clinic Foundation and Cleveland State University

Follow this and additional works at: https://engagedscholarship.csuohio.edu/encbe_facpub

 Part of the [Biochemical and Biomolecular Engineering Commons](#), and the [Biomedical Engineering and Bioengineering Commons](#)

How does access to this work benefit you? Let us know!

Original Citation

Journal of Cardiovascular Magnetic Resonance (2005) 7, 573–579

Repository Citation

Kolipaka, Arunark; Chatzimavroudis, George P.; White, Richard D.; Lieber, Michael L.; and Setser, Randolph M., "Relationship between the extent of non-viable myocardium and regional left ventricular function in chronic ischemic heart disease" (2005). *Chemical & Biomedical Engineering Faculty Publications*. 29.
https://engagedscholarship.csuohio.edu/encbe_facpub/29

This Article is brought to you for free and open access by the Chemical & Biomedical Engineering Department at EngagedScholarship@CSU. It has been accepted for inclusion in Chemical & Biomedical Engineering Faculty Publications by an authorized administrator of EngagedScholarship@CSU. For more information, please contact library.es@csuohio.edu.

MYOCARDIAL VIABILITY

Relationship between the extent of non-viable myocardium and regional left ventricular function in chronic ischemic heart disease

ARUNARK KOLIPAKA,^{1,2} GEORGE P. CHATZIMAVROUDIS,^{1,2} RICHARD D. WHITE,¹ MICHAEL L. LIEBER,³ and RANDOLPH M. SETSER, D.Sc.^{1,2,*}

¹Section of Cardiovascular Imaging, Division of Radiology, The Cleveland Clinic Foundation, Cleveland, Ohio, USA

²Department of Chemical and Biomedical Engineering, Cleveland State University, Cleveland, Ohio, USA

³Department of Biostatistics and Epidemiology, The Cleveland Clinic Foundation, Cleveland, Ohio, USA

Purpose. To define the relationship between left ventricular (LV) regional contractile function and the extent of myocardial scar in patients with chronic ischemic heart disease and multi-vessel coronary artery disease. **Methods.** Twenty-three patients with chronic ischemic heart disease and 5 healthy volunteers underwent magnetic resonance imaging (MRI). In patients, the relative area (Percent Scar) and transmural extent (Transmurality) of myocardial infarction were computed from short-axis delayed enhancement images. In each image, myocardial segments were categorized based on the extent of infarction they contained, with 6 categories each for Percent Scar and Transmurality: normal, from healthy volunteers; and 0%; 1–25%, 26–50%, 51–75%, and > 76% from patients. In patients and volunteers, regional LV function was quantified by absolute systolic wall thickening from cine images and midwall circumferential strain using tagged images. **Results.** Compared to normal segments, regional LV function in patients was significantly diminished in all scar extent intervals, with wall thickening ≤ 1 mm and strain $\geq -8\%$ for all categories. Systolic wall thickening was reduced significantly in all categories above 50% Percent Scar and above 25% Transmurality in patients, relative to corresponding 0% categories. Circumferential strain was significantly reduced above 25% Percent Scar and above 25% Transmurality. **Conclusions.** In patients with chronic ischemic heart disease and multi-vessel coronary artery disease, wall thickening was more sensitive to changes in scar Transmurality than to changes in Percent Scar. However, circumferential strain was equally sensitive to both indices. In general, circumferential strain was more sensitive than wall thickening to increases in scar extent.

Key Words: Ischemic heart disease; Left ventricular function; Wall thickening; Circumferential strain; Delayed enhancement MRI; HARP

1. Introduction

Ischemic heart disease is the leading cause of chronic heart failure in western society (1, 2). However, its effects on cardiac function are not uniform, as the degree of dysfunction varies with the relative quantities of ischemic, hibernating, and infarcted myocardium in the left ventricle (LV). Furthermore, the effects of ischemic heart disease are exacerbated by LV remodeling and dilatation as the disease progresses (1).

Magnetic resonance imaging (MRI) has proven a valuable tool for quantifying the impact of ischemic heart disease (3). The extent of non-viable myocardium can be directly visualized using delayed enhancement (DE) MRI (4, 5). Fur-

thermore, other MRI techniques enable assessment of LV wall motion, intramyocardial mechanics, or myocardial perfusion in order to differentiate regions of myocardium that are normal, inducibly ischemic, chronically ischemic (e.g. hibernating) or infarcted (3).

The relationship between the extent of non-viable LV myocardium and regional cardiac function has been studied previously in the setting of single-vessel coronary artery disease (6, 7). In a dog model of acute myocardial infarction, Lieberman et al. demonstrated an abrupt deterioration of systolic wall thickening in segments with more than 20% transmural extent of infarction (6). In a separate study, involving patients with reperfused chronic infarcts, Mahrholdt et al. (7) determined that systolic wall thickening was diminished in segments containing more than 50% non-viable myocardium. However, the relationship between the extent of non-viable tissue and regional cardiac function in patients presenting with multi-vessel chronic ischemic heart disease has not been studied.

The purpose of the current study was to examine the relationship between scar extent and regional myocardial

Received 22 May 2004; accepted 14 February 2005.

*Address correspondence to Randolph M. Setser, D.Sc., Section of Cardiovascular Imaging, Division of Radiology, Desk Hb6, The Cleveland Clinic Foundation, 9500 Euclid Ave., Cleveland, OH 44195, USA; Fax: (216) 445-1492; E-mail: setserr@ccf.org

function in patients with chronic ischemic heart disease and multi-vessel coronary artery disease and to determine if the relationship between scar and function is preserved, even with the confounding effects of myocardial ischemia and hibernation. Further, the authors sought to determine whether circumferential strain would be more sensitive than wall thickening to the presence of myocardial scar in this population as it has been previously established in patients with acute myocardial infarction (8).

2. Materials and methods

2.1. Patient population

The study population consisted of 23 patients (20 male/3 female; age 59 ± 13 years) with known chronic ischemic heart disease, referred for MRI assessment of myocardial viability. All patients had a history of hemodynamically significant atherosclerotic coronary artery disease, defined by the presence of at least one coronary stenosis $> 50\%$. Most patients (22 of 23; 96%) had multi-vessel coronary artery disease (2 vessels: $n = 4$, 17%; 3 vessels: $n = 18$, 78%). The lone patient with single-vessel disease (left anterior descending artery) also had 20–30% stenoses in both the circumflex and right coronary arteries as well as non-viable myocardium present in territories supplied by these arteries (visualized using DE-MRI). No patient presented with acute myocardial infarction. All patients had previously documented congestive heart failure symptoms; at the time of MRI, New York Heart Association functional class was distributed as follows: class I ($n = 2$, 9%), class II ($n = 10$, 43%), class III ($n = 8$, 35%), class IV ($n = 3$, 13%). All imaging studies were clinically indicated; further image analysis, for research purposes, was approved by the local Institutional Review Board with a waiver of individual consent.

In addition, five healthy volunteers, all men (age 23 ± 1 years), with no prior history of heart disease were also imaged.

2.2. Imaging procedure

Imaging was performed using a 1.5 T MRI scanner (Sonata, Siemens Medical Solutions, Erlangen, Germany).

Short-axis DE-MRI images were acquired at the basal, middle, and apical thirds of the LV, approximately 20 minutes after intravenous injection of 0.2 mmol/kg Gadolinium-DTPA (Magnevist, Berlex, Laboratories, Wayne, NJ). Fourteen of 23 patients (61%) were imaged using an inversion recovery TurboFLASH sequence (4). The remaining 9 patients (39%) were imaged using an inversion recovery TurboFlash sequence with phase sensitive reconstruction (9). The imaging parameters for either sequence included TE 4 msec, TR 8 msec, flip angle 30° , TI 190–470 msec, 23 lines acquired every other RR-interval, slice thickness 8–10 mm, FOV 300–360 mm, RFOV 80–100%, NSA 1, initial matrix 256^2 , and a breath hold of 10–15 sec, depending upon the heart rate.

Cine MRI image loops were acquired at short-axis levels covering the LV in each patient using a balanced steady state free precession pulse sequence (TrueFISP). Imaging parameters included TE 1.5–1.65 msec, TR 25–43 msec, flip angle $49\text{--}65^\circ$, slice thickness either 6 or 10 mm, FOV_x 263–360 mm, FOV_y 300–360 mm, initial matrix 256^2 . The breath hold was 10–15 sec depending on the heart rate.

Tagged MRI image loops were acquired in each patient using a segmented TurboFLASH sequence at short-axis levels identical to those specified for DE imaging above. Imaging parameters included TE 2.7–4.8 msec, TR 25–66 msec, flip angle $14\text{--}30^\circ$, slice thickness 6–10 mm, FOV_x 244–350 mm, FOV_y 300–380 mm, initial matrix 256^2 . Each breath hold was 15–20 sec depending on heart rate.

In each healthy volunteer, short-axis cine MR image loops and tagged image loops were acquired at the basal, middle and apical thirds of the LV, using acquisition sequences identical to those described above for patient imaging. However, DE-MRI was not performed in volunteers.

2.3. Image analysis

2.3.1. Quantitative analysis of DE images

Epicardial and endocardial contours were drawn manually in each short-axis DE image using cardiovascular image analysis software (Argus, Siemens Medical Solutions, Erlangen, Germany). Images were then manually thresholded with custom analysis software (modified Argus, Siemens Medical Solutions, Erlangen, Germany) using an interactive region-filling tool to determine an appropriate intensity threshold to differentiate viable (dark) from non-viable (hyper-enhanced) tissue in each image (10).

Analysis of thresholded images was performed using Matlab (v6.5, The MathWorks, Natick, MA, USA). Regional variations in myocardial scar extent were examined using a 16-segment LV model (11). Percent Scar was defined as the ratio of the number of non-viable pixels to the total number of pixels within each segment. Transmurality was defined as the average extent to which non-viable pixels originating at the subendocardium traversed the LV wall in each segment (10), and was computed in each thresholded image by analyzing 180 equiangular radial spokes centered at the LV center of volume in that slice. For spokes in which non-viable pixels originated at the subendocardium, Transmurality was computed as the ratio of non-viable pixels to total pixels along the spoke. Transmurality within a segment was defined as the average of all spokes within that segment.

2.3.2. Quantitative analysis of cine MRI

Epicardial and endocardial borders were manually delineated in cine MRI short axis images at end-diastole and end-systole (using Argus software, Siemens Medical Solutions, Erlangen, Germany). LV wall thickness at each time point was computed using the centerline method (12). Absolute systolic wall thickening was computed as the difference between

end-systolic wall thickness and end-diastolic wall thickness. Regional wall thickening was defined using the 16-segment LV model described above.

2.3.3. Quantitative analysis of tagged images

LV circumferential strain was computed using harmonic phase (HARP) analysis software (Diagnosoft, CA, USA) (13). Briefly, HARP utilizes isolated spectral peaks in the frequency-domain representation of tagged images. The inverse Fourier transform of a spectral peak yields a complex image whose phase is related to cardiac motion in one direction. Analysis of two spectral peaks enables two-dimensional cardiac motion to be determined, including tracking individual points within the myocardium. The LV mid-wall was specified by manually delineating the endocardium and epicardium at end-systole at each short-axis level; the mid-wall was then located automatically in all other frames. Points lying on the mid-wall contour were tracked automatically by the HARP software from end-diastole to end-systole. LV circumferential strain in each short-axis image was calculated based on the average motion of mid-wall points. Regional circumferential strain was defined using the 16-segment LV model defined above.

2.4. Data analysis

Results for each scar extent variable (Percent Scar and Transmurality) from patient images were grouped into five categories: 0%; 1%–25%; 26%–50%; 51%–75%; and 76%–100%. Segments from healthy volunteer images served as a sixth category (normal). Average systolic wall thickening and average circumferential strain were computed for the segments in each category.

One-way analysis of variance with Tukey's pairwise comparison (14) was used to determine the significance of differences between myocardial scar categories. Paired student's *t*-test was used to assess differences between Percent Scar and Transmurality in all patient segments.

Linear mixed-model statistical methods (15) were used to assess the significance of Percent Scar and Transmurality in explaining regional variations in LV function (systolic wall thickening and circumferential strain). Each measure of function was modeled separately, with both Percent Scar and Transmurality included in each model as potential predictors.

Results are presented as mean \pm standard deviation. In all figures, error bars represent standard deviation.

3. Results

All patients demonstrated increased LV dimensions (end-diastolic volume: 274 ± 11 ml) and impaired systolic function (ejection fraction: $28 \pm 11\%$, cardiac output of 5 ± 1 l/min). Table 1 shows the end-diastolic volume, ejection fraction, and cardiac output for each patient.

Table 1. Clinical characteristics of each patient

Patient	Gender	Age (years)	EDV(ml)	EF(%)	CO (l/min)
1	M	59	321	17	4.2
2	M	47	198	33	4.3
3	M	39	341	23	5.7
4	M	54	307	30	6.2
5	M	68	183	45	5.4
6	M	64	412	19	6.6
7	M	58	350	17	4.7
8	F	68	171	17	2.6
9	M	48	277	22	5.7
10	M	54	247	22	4.3
11	M	73	231	34	4.3
12	M	45	389	09	2.7
13	F	43	154	32	5.0
14	M	67	334	31	7.7
15	M	29	259	48	7.7
16	M	71	193	56	7.2
17	M	64	332	26	6.9
18	M	72	363	12	3.9
19	M	65	244	25	4.0
20	F	55	202	29	4.5
21	M	72	235	32	4.5
22	M	75	351	22	4.8
23	M	72	205	36	4.4
Average		59 ± 13	274 ± 76	28 ± 11	5.1 ± 1.4

Gender, age (years), end-diastolic volume (EDV), ejection fraction (EF), and cardiac output (CO). Also shown is the mean value (\pm standard deviation) of each applicable parameter.

3.1. Relationship between scar extent and systolic wall thickening

Figure 1A is a scatterplot of wall thickening versus Percent Scar for all 368 segments from patient images (23 patients \times 16 segments, does not include segments from healthy volunteers). Average systolic wall thickening within each Percent Scar category is shown in Fig. 2, and average systolic wall thickening within each Transmurality category is shown in Fig. 3. Relative to normal segments, systolic wall thickening was significantly reduced in all Percent Scar and Transmurality categories containing patient data (0%; 1–25%; 26–50%; 51–75%; and 76–100%).

In patients, systolic wall thickening was significantly reduced above 50% Percent Scar, relative to the 0% category (Fig. 2). However, systolic wall thickening was significantly reduced above 25% Transmurality, relative to the 0% category (Fig. 3). Although the 76–100% Transmurality category did not differ significantly from segments without scar (0%), the number of segments with 76–100% Transmurality was small ($n = 8$; 2%) when compared to the number with 0% scar ($n = 130$; 35%).

In a linear mixed-model regression of wall thickening, which incorporated the effects of both Percent Scar and Transmurality, neither of these scar variables was statistically

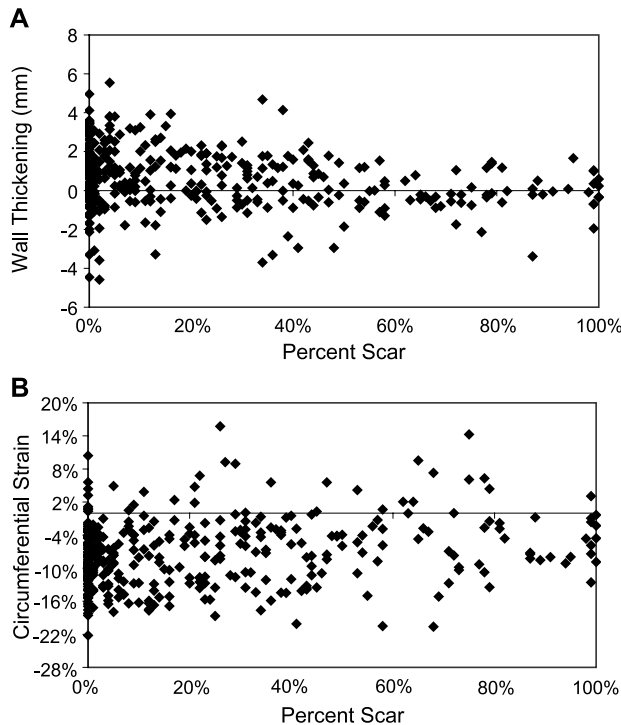


Figure 1. (A) Overall effects of Percent Scar on absolute systolic wall thickening in all segments taken from patient images ($n = 368$). Despite the apparent spread in the data, wall thickening decreased significantly as Percent Scar increased (see text for details). (B) Overall effects of Percent Scar on circumferential strain in all segments taken from patient images. Circumferential strain worsened significantly (became less negative) as Percent Scar increased.

significant: $p = 0.15$ for Percent Scar, $p = 0.73$ for Transmurality. However, when considered alone, Percent Scar was a statistically significant predictor of wall thickening ($p < 0.0001$, Fig. 1A). Similarly, Transmurality was a significant predictor of wall thickening when considered alone ($p < 0.001$).

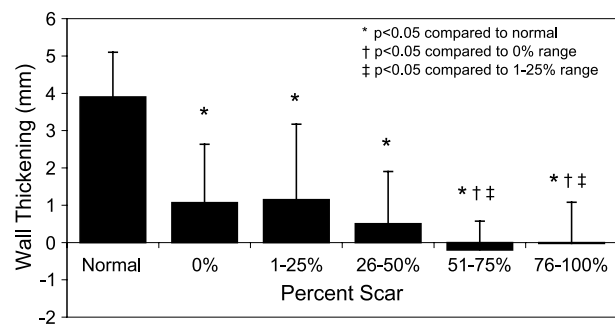


Figure 2. Average systolic wall thickening within each of the six Percent Scar categories: normal from healthy volunteers and the remaining categories from patient images.

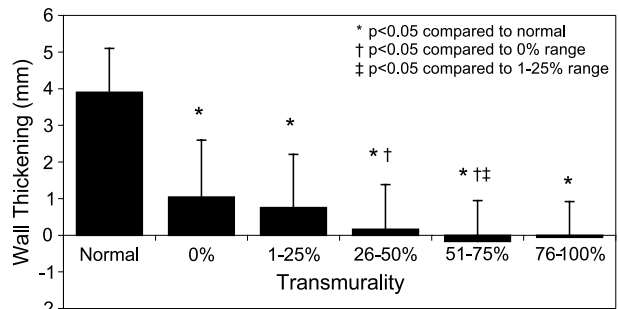


Figure 3. Average systolic wall thickening within each of the six Transmurality categories: normal from healthy volunteers and the remaining categories from patient images.

3.2. Relationship between scar extent and circumferential strain

A scatterplot of circumferential strain as a function of Percent Scar for all 368 patient segments is displayed in Fig. 1B. Circumferential strain within each Percent Scar category is shown in Fig. 4, and circumferential strain within each Transmurality category is shown in Fig. 5. Relative to Normal segments, circumferential strain was significantly reduced in all Percent Scar and Transmurality categories containing patient data.

In patients, circumferential strain was significantly reduced above 25% Percent Scar (Fig. 4). Similarly, circumferential strain was significantly reduced above 25% Transmurality (Fig. 5). However, as with wall thickening, the 76–100% Transmurality category did not differ significantly from the 0% category, although the number of segments in this Transmurality category was small ($n = 8$ of 368, 2%) when compared to the number with 0% scar ($n = 130$, 35%).

In a linear mixed-model regression of circumferential strain on the combined effects of Percent Scar and Transmurality, Percent Scar was statistically significant ($p = 0.035$, Fig. 1B), but Transmurality was not ($p = 0.77$), with the resultant model described by the equation, circumferential

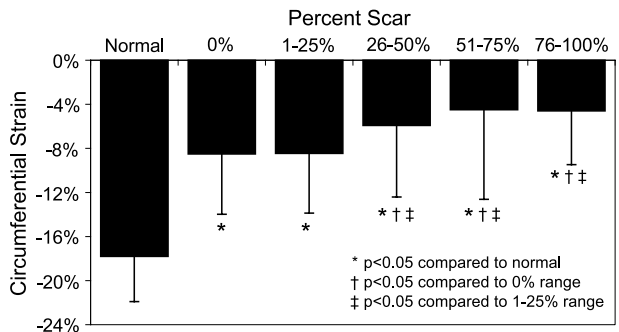


Figure 4. Average circumferential strain within each of the six Percent Scar categories: normal from healthy volunteers and the remaining categories from patient images.

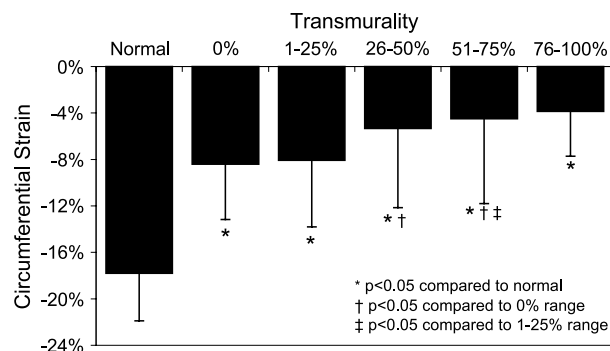


Figure 5. Average circumferential strain within each of the six Transmurality categories. The normal category represents data from healthy volunteers, and the remaining categories from patient images.

strain = $-8.6 + 0.067^*(\text{Percent Scar}) - 0.013^*(\text{Transmurality})$. Similar to the wall thickening analysis, when considered alone in a separate model, Transmurality became a statistically significant predictor of circumferential strain ($p = 0.003$).

4. Discussion

In patients with chronic ischemic heart disease, regional LV function is influenced by numerous factors, including the presence of ischemic or hibernating myocardium and elevated wall stress secondary to LV remodeling and heart failure (1). Thus, it is not surprising that in the current study, we have observed diminished regional LV function, as quantified by either wall thickening or circumferential strain, even in segments containing little or no non-viable myocardium (Fig. 1A and 1B). Similarly, the myocardial segments in all scar extent categories (0%; 1–25%; 26–50%; 51–75%; and 76–100%) demonstrated significantly impaired regional systolic function (Figs. 2–5), with mean wall thickening ≤ 1 mm and mean circumferential strain $\geq -8\%$ in all categories, when compared with segments containing only healthy myocardium (normal); these results are consistent with a recently published study (16).

Alternate imaging studies were available for comparison in 12 of 23 patients (52%), including rubidium (Rb) positron emission tomography (PET) stress perfusion with fluorodeoxyglucose (FDG) viability imaging ($n = 9$; 39%), stress myocardial perfusion single photon emission computed tomography (SPECT) ($n = 2$; 9%), and stress echocardiography ($n = 1$; 4%). By these modalities, 11 of 12 patients (92%) exhibited non-viable myocardial segments (one patient with scar by MRI was judged to have none by SPECT). In addition, 4 of 12 patients (33%) exhibited ischemic segments, which were estimated to cover 4–30% of the LV, and 1 patient (8%) exhibited hibernating segments, estimated to cover 6% of the LV. Six patients (50%) had neither ischemic nor hibernating segments, as assessed by these alternate

imaging modalities. Thus, at least in this subset of patients, regional LV dysfunction could be attributed to the spectrum of causes common to chronic ischemic heart disease.

4.1. Relationship between scar extent and systolic wall thickening

Two previous studies have examined the relationship between scar extent and regional LV function in subjects with single-vessel coronary artery disease and have reported findings similar to those of the current work. In a dog model of acute myocardial infarction, Lieberman et al. showed reduced segmental wall thickening when scar transmurality exceeded 20% (6). In a study of patients with single vessel coronary disease and chronic infarcts studied an average of 5 months post-revascularization, Marholdt et al. found significantly reduced wall thickening in segments containing at least 50% scar (7). Although these results seem disparate, their findings closely mirror those of the current study, in which systolic wall thickening was found to be significantly diminished in segments with greater than 25% Transmurality or greater than 50% Percent Scar, relative to corresponding 0% categories (Figs. 2 and 3). In their work, Lieberman et al. measured the average transmural extent of infarction, identical to the Transmurality index described in the current study, and their results matched those of the current study using Transmurality. Marholdt et al., meanwhile, measured the relative area of scar in each segment, identical to Percent Scar from the current study (although they referred to their measurements as transmurality); their results matched those of the current study for Percent Scar. Therefore, discrepancies between these previous studies might merely reflect differences in the parameters they measured, although the differences in population (dog versus human) and infarct age (acute versus chronic) are also potential factors.

In this study, the range of wall thickening values exhibited by normal segments, i.e. those from healthy volunteers, was consistent with that of previous studies, which have reported values from 4–7 mm depending on modality (17–21). Furthermore, 303 of the 368 patient segments (82%) exhibited absolute wall thickening < 2 mm, which has been used previously as a threshold for discriminating normal from hypokinetic segments (22, 23). In the remaining 65 patient segments (18%), wall thickening was 2.9 ± 0.8 mm.

The use of absolute systolic wall thickening by the current study was a departure from similar previous studies, which have reported relative wall thickening (6, 7). However, due to the thin LV wall (mean end-diastolic thickness 6.8 ± 2.1 mm) and diminished wall thickening (< 1 image pixel width on average) exhibited by patients in this study, we felt that relative thickening results would be misleading, in part because small errors in delineating the myocardium could lead to large errors in relative wall thickening. For example, 100 of 368 patient segments (27%) had an end-diastolic wall

thickness < 5.5 mm, which has been used previously as a threshold for the absence of viability (24, 25); in these segments, mean systolic wall thickening was 0.9 ± 1.2 mm ($18 \pm 25\%$). In the remaining 268 segments (73%), i.e. those with end-diastolic thickness ≥ 5.5 mm, mean systolic wall thickening was 0.6 ± 1.6 mm ($9 \pm 21\%$). The difference between these groups was not statistically significant for absolute thickening ($p = 0.26$) but was statistically significant for relative thickening ($p = 0.001$). Thus, relative thickening underestimated the degree of dysfunction in the thinnest segments.

In a linear mixed-model analysis, neither Percent Scar nor Transmurality were statistically significant predictors of systolic wall thickening when both variables were included in the model; however, each was significant when considered alone in a separate model. This suggests that these variables contribute redundant information with neither one standing out as a superior predictor of wall thickening as a measure of regional function.

4.2. Relationship between scar extent and circumferential strain

Percent Scar and Transmurality affected circumferential strain similarly, with significant reductions in strain when either scar extent index exceeded 25% (Figs. 4 and 5). Although these results are similar to those for wall thickening, circumferential strain proved to be a more sensitive marker of increases in Percent Scar, as demonstrated by Figs. 2 and 4. This finding is consistent with a previous report, which showed circumferential strain to be more sensitive to the presence of myocardial infarction than wall thickening (8).

In a linear mixed-model analysis including both Percent Scar and Transmurality as potential predictors of circumferential strain, only Percent Scar was statistically significant. Thus, at least in this type of analysis, this suggests that Percent Scar is more predictive of strain than Transmurality.

Close inspection of the model equation for strain, presented in the Results section, demonstrates that strain actually improves (becomes more negative) when Transmurality is nonzero. For example, considering two hypothetical segments each with 50% Percent Scar, if the scar originates at the subendocardium (i.e. nonzero Transmurality by our definition), strain will be improved relative to a segment in which the scar does not originate at the subendocardium (i.e. Transmurality zero).

5. Conclusions

In patients with ischemic heart disease and multi-vessel coronary artery disease, the relationship between myocardial scar extent and regional LV function is consistent with that reported previously in studies of subjects with single-vessel disease. However, this relationship exhibits more variability

in multi-vessel disease patients due to the multiple confounding factors associated with ischemic heart disease (e.g. hibernating myocardium).

In this population, wall thickening is more sensitive to changes in Transmurality than to changes in Percent Scar, but circumferential strain shows equal sensitivity to both scar extent indices. Furthermore, in general, circumferential strain is more sensitive than wall thickening to increases in scar extent.

Acknowledgments

This work was presented at the SCMR 7th annual scientific meeting, 2004.

We would like to thank Angel Lawrence, R.T., for scanning the healthy volunteers. We would also like to acknowledge Jim Williams, Ph.D., and Siemens Corporate Research (Princeton, NJ) for partially supporting this work (AK).

References

1. Gheorghiade M, Bonow RO. Chronic heart failure in the United States: a manifestation of coronary artery disease. *Circulation* 1998; 97:282–289.
2. Stewart S, MacIntyre K, Capewell S, McMurray JJV. Heart failure and the aging population: an increasing burden in the 21st century? *Heart* 2003; 89:49–53.
3. Schartzmann PR, White RD. Magnetic resonance imaging. In: Topol EJ, ed. *Textbook of Cardiovascular Medicine*. 2nd ed. 2002. Philadelphia: Lippincott Williams and Wilkins, 1213–1256.
4. Simonetti OP, Kim RJ, Fieno DS, Hillenbrand HB, Edwin W, Burdy JM, Paul Finn J, Judd RM. An improved MR imaging technique for the visualization of myocardial infarction. *Radiology* 2001; 218:215–223.
5. Fieno DS, Kim RJ, Chen EL, Lomasney JW, Klocke FJ, Judd RM. Contrast-enhanced magnetic resonance imaging of myocardium at risk: distinction between reversible and irreversible injury throughout infarct healing. *J Am Coll Cardiol* 2000; 36:1985–1991.
6. Lieberman AN, Weiss JL, Jugdutt BI, Becker LC, Bulkley BH, Garrison JG, Hutchins GM, Kallman CA, Weisfeldt ML. Two-dimensional echocardiography and infarct size: relationship of regional wall motion and thickening to the extent of myocardial infarction in the dog. *Circulation* 1981; 63:739–746.
7. Mahrholdt H, Wagner A, Parker M, Regenfus M, Fieno DS, Bonow RO, Kim RJ, Judd RM. Relationship of contractile function to transmural extent of infarction in patients with chronic coronary artery disease. *J Am Coll Cardiol* 2003; 42:505–512.
8. Götte MJW, van Rossum AC, Twisk JWR, Kuijper JPA, Marcus T, Visser CA. Quantification of regional contractile function after infarction: strain analysis superior to wall thickening analysis in discriminating infarct from remote myocardium. *J Am Coll Cardiol* 2001; 37:808–817.
9. Kellman P, Arai AE, McVeigh ER, Haletas A. Phase-sensitive inversion recovery for detecting myocardial infarction using gadolinium delayed hyperenhancement. *Magn Reson Med* 2002; 47:372–383.
10. Setser RM, Bexell DG, O'Donnell TP, Stillman AE, Lieber ML, Schoenhagen P, White RD. Quantitative assessment of myocardial scar in delayed-enhancement magnetic resonance imaging. *J Magn Reson Imaging* 2003; 18:434–441.

11. Schiller NB, Shah PM, Crawford M. Recommendations for quantification of the left ventricle by two-dimensional echocardiography. *J Am Soc Echocardiogr* 1989; 2:358–367.
12. van Ruge FP, van der Wall EE, Spanjersberg SJ, Albert de Ross, Matheijssen NAA, Zwinderman AH, van Dijkman PRM, Reiber JHC, Bruschke AVG. Coronary heart disease/myocardial infarction: magnetic resonance imaging during dobutamine stress for detection and localization of coronary artery disease: quantitative wall motion analysis using a modification of the centerline method. *Circulation* 1994; 90:127–138.
13. Osman NF, Kerwin WAS, McVeigh ER, Prince JL. Cardiac motion tracking using CINE harmonic phase (HARP) magnetic resonance imaging. *Magn Reson Med* 1999; 42:1048–1060.
14. Glantz SA. *Primer of Biostatistics*. 5th ed. New York: McGraw-Hill, 2002.
15. Crowder MJ, Hand DJ. *Analysis of Repeated Measures*. London: Chapman & Hall, 1990.
16. Srichai MB, Schwartzman PR, Sturm B, Kasper JM, Lieber ML, White RD. Extent of myocardial scarring on nonstress delayed-contrast-enhancement cardiac magnetic resonance imaging correlates directly with degrees of resting regional dysfunction in chronic ischemic heart disease. *Am Heart J* 2004; 148:342–348.
17. Sehgal M, Hirose K, Reed JE, Rumberger JA. Regional left ventricular wall thickness and systolic function during the first year after index anterior wall myocardial infarction: serial effects of ventricular remodeling. *Int J Cardiol* 1996; 53:45–54.
18. Fisher MR, von Schulthess GK, Higgins CB. Multiphasic magnetic resonance imaging: normal regional left ventricular wall thickening. *AJR* 1985; 145:27–30.
19. Sechtem U, Sommerhoff BA, Markiewicz W, White RD, Cheitlin MD, Higgins CB. Regional left ventricular wall thickening by magnetic resonance imaging: evaluation in normal persons and patients with global and regional dysfunction. *Am J Cardiol* 1987; 59:145–151.
20. Peshock RM, Rokey R, Malloy CM, McNamee P, Maximilian Buja L, Parkey RW, Willerson JT. Assessment of myocardial systolic wall thickening using nuclear magnetic resonance imaging. *J Am Coll Cardiol* 1989; 14:653–659.
21. Frielingsdorf J, Franke A, Kuhl HP, Rijcken E, Krebs W, Hess OM, Flachskampf FA, Hanrath P. Evaluation of regional systolic function in hypertrophic cardiomyopathy and hypertensive heart disease: a three-dimensional echocardiography study. *J Am Soc Echocardiogr* 1998; 11:778–786.
22. Sechtem U, Sommerhoff BA, Markiewicz W, White RD, Cheitlin MD, Higgins CB. Regional left ventricular wall thickening by magnetic resonance imaging: evaluation in normal persons and patients with global and regional dysfunction. *Am J Cardiol* 1987; 59:145–151.
23. Perrone-Filardi P, Bacharach SL, Dilsizian V, Maurea S, Frank JA, Bonow RO. Regional left ventricular wall thickening: relation to regional uptake of ^{18}F fluorodeoxyglucose and ^{201}Tl in patients with chronic coronary artery disease and left ventricular dysfunction. *Circulation* 1992; 86:1125–1137.
24. Baer FM, Voth E, Schneider CA, Theissen P, Schisha H, Sechtem U. Comparison of low-dose dobutamine-gradient-echo magnetic resonance imaging and positron emission tomography with [^{18}F]fluorodeoxyglucose in patients with chronic coronary artery disease. A functional and morphological approach to the detection of residual myocardial viability. *Circulation* 1995; 91:1006–1015.
25. Baer FM, Theissen P, Schneider CA, Voth E, Sechtem U, Schisha H, Erdmann E. Dobutamine magnetic resonance imaging predicts contractile recovery of chronically dysfunctional myocardium after successful revascularization. *J Am Coll Cardiol* 1998; 31:1040–1048.

Copyright of Journal of Cardiovascular Magnetic Resonance is the property of Marcel Dekker Inc. and its content may not be copied or emailed to multiple sites or posted to a listserv without the copyright holder's express written permission. However, users may print, download, or email articles for individual use.